Combined ^{18}F-FDG PET/CT imaging and a gastric orthotopic xenograft model in nude mice are used to evaluate the efficacy of glycolysis-targeted therapy

TING-AN WANG*, SHU-LIN XIAN*, XING-YU GUO, XIAO-DONG ZHANG and YUN-FEI LU

Department of Gastrointestinal and Gland Surgery, The First Affiliated Hospital of Guangxi Medical University, Nanning, Guangxi 530021, P.R. China

Received November 19, 2016; Accepted June 22, 2017

DOI: 10.3892/or.2017.6060

Abstract. As discovered by Warburg 80 years ago most malignant cells rely more on glycolysis than normal cells. The high rate of glycolysis provides faster ATP production and greater lactic acid for tumor proliferation and invasion, thus indicating a potential target in anticancer therapy. Our previous studies demonstrated that 3-bromopyruvate (3-BrPA) and sodium citrate (SCT) inhibited tumor cell proliferation *in vitro*. However, the underlying mechanisms still warrant further investigation. In the present study, we employed the human SGC-7901 gastric cancer cell line, built an orthotopic xenograft model in nude mice, examined the treatment response by ^{18}F-FDG PET/CT and investigated the mechanisms of 3-BrPA and SCT *in vivo*. Our results demonstrated that glycolysis and tumor growth were inhibited by intraperitoneal injection of 3-BrPA and SCT, which were imaged using an ^{18}F-FDG PET/CT scanner. In addition, apoptosis induced by 3-BrPA and SCT was initiated by the upregulation of Bax and downregulation of Bcl-2, which promote cytochrome *c* release and subsequently activate caspase-9 and -3, and ultimately execute mitochondria-mediated apoptosis. Furthermore, apoptosis was also modulated by the generation of ROS and inhibition of survivin. Accordingly, 3-BrPA and SCT can inhibit glycolysis and induce gastric cancer apoptosis through the mitochondrial caspase-dependent pathway.

Correspondence to: Dr Xiao-Dong Zhang or Professor Yun-Fei Lu, Department of Gastrointestinal and Gland Surgery, The First Affiliated Hospital of Guangxi Medical University, 6 Shuangyong Road, Nanning, Guangxi 530021, P.R. China
E-mail: 1039134280@qq.com
E-mail: doctorlife@126.com

*Contributed equally

Key words: micro-PET/CT, glycolysis, gastric cancer, orthotopic xenograft, apoptosis

Introduction

Despite advances in surgical techniques, adjuvant chemotherapy, radiotherapy and immune therapy in the past decades, cancer is still the second leading cause of death worldwide alongside heart diseases (1). In particular, gastric cancer (GC), with the highest prevalence in Eastern Asia (including Japan, Korea and China) worldwide, has a 5-year survival rate of less than 30% (1,2). Therefore, the discovery of novel and more effective therapeutic targets against cancer appears to be of central importance.

In 1956, Otto Warburg observed that malignant cells undergo a higher rate of glycolysis for energy in contrast to healthy cells (3). Based on this characteristic of cancer cells, 2'-[^{18}F]-fluoro-2'-deoxy-D-glucose positron emission tomography (^{18}F-FDG PET) has been extensively used to diagnose and assess various cancers including GC, and the changes in ^{18}F-FDG uptake can also reflect early treatment response (4,5). In addition, this glycolytic metabolic characteristic of cancer cells also suggests that targeting glycometabolism may be an effective way to selectively inhibit cancer cells (6). Moreover, this dysregulated metabolism has been revealed to promote drug resistance in malignant cells (7).

Recently, a number of molecules have been discovered to suppress glycolysis in cancer cells. Various representative drugs are iodoacetic acid (IAA), dichloroacetate (DCA), 2-deoxyglucose and 3-bromopyruvate (3-BrPA). Previous studies from Pedersen and our team revealed that 3-BrPA decreased glycolysis by suppressing mitochondrial hexokinase activity (8,9). Similarily, sodium citrate (SCT), a member of the mitochondrial tricarboxylic acid cycle, has also been revealed to inhibit medullary thyroid cancer, leucocythemia, malignant pleural mesothelioma and ovarian carcinoma growth (10-13).

It is generally known that the potential anticancer ability of a new therapeutic approach is often evaluated by activation of tumor cell apoptosis. There are 2 major signaling pathways that induce apoptosis: the extrinsic (death receptor) pathway mediated by procaspase-8, and the intrinsic (mitochondrial) pathway which is triggered by the disruption of the mitochondrial transmembrane potential, release of apoptogenic

proteins such as cytochrome *c* (Cyt-C) into the cytoplasm and subsequent activation of caspase-9 (14-16). The 2 signaling pathways converge at the activation of caspase-3, a key mediator in the execution apoptosis (17). Furthermore, the proteins in the Bcl-2 family such as pro-apoptotic Bax and anti-apoptotic Bcl-2, modulate the mitochondrial membrane potential thus regulating apoptotic signaling (18). In addition, as a member of the IAP family, survivin is abundantly expressed in the majority of human cancers, and is associated with tumor proliferation and treatment resistance (19). Survivin inhibits the activation of caspases and is a target of anticancer drugs (20,21). Moreover, reactive oxygen species (ROS) generated in and around mitochondria, has been indicated to induce uncontrolled oxidative stress and subsequent cell apoptosis (22).

The application of tumor animal models is extremely important in pre-clinical studies of oncology (23), and traditional ectopic models were restricted in their poor representation of the pathophysiological milieu around tumors (24). Thus, it is necessary to create practicable orthotopic xenograft tumor models that mimic the biological characteristics of human tumors in order to discover successful therapeutic strategies (25).

The results from our previous studies indicated that the antitumor mechanisms of 3-BrPA and SCT warrant further investigation (9,13). In the present study, we created a GC orthotopic xenograft model in nude mice and intraperitoneally injected 3-BrPA and SCT. The antitumor efficacy of 3-BrPA and SCT was detected using a micro-PET/CT scanner. We also explored the underlying mechanisms in the inhibition of tumors induced by 3-BrPA and SCT. In the present study the results demonstrated that the antitumor effect was associated with the generation of ROS, upregulation of Bax, downregulation of Bcl-2 and survivin, release of Cyt-C and activation of caspase-3 and -9 cascades.

Materials and methods

Cell line and reagents. Gastric carcinoma cell line SGC-7901 was purchased from the Cell Bank of the Chinese Academy of Sciences (Shanghai, China). The cell line was maintained in RPMI-1640 medium supplemented with 10% fetal calf serum (Gibco, Carlsbad, CA, USA), 100 U/ml penicillin and 100 μg/ml streptomycin, in a humidified atmosphere with 5% CO_2 at 37˚C.

3-BrPA, SCT and 5-fluorouracil (5-FU) were purchased from Sigma-Aldrich (St. Louis, MO, USA), dissolved in medium and phosphate-buffered saline (PBS) to create working solutions and filtered and sterilized prior to treatment.

Cell proliferation assay. In order to determine the sensitivity of the SGC-7901 cell line to 3-BrPA, SCT or 5-FU, ~2,000 cells were seeded into 96-well plates and exposed to varying concentrations of the drugs for 24 and 48 h. Then, the cells were incubated with 10 μl of 5 mg/ml 3-(4,5-demethylthiazol-2-yl)-2,5-diphenyltetrazonium bromide (MTT) for a further 4-h incubation at 37˚C. Dimethyl sulfoxide (DMSO) was added to each well, and was shaken for 30 sec. The absorbance at 490 nm was quantified using a microplate reader (Bio-Rad, Hercules, CA, USA).

Hochest 33258 staining. To detect apoptosis *in vitro*, SGC-7901 cancer cells were grown in 6-well plates and treated with 3-BrPA, SCT and 5-FU for 24 h, then stained with Hochest 33258 (Beyotime Biotechnology, Jiangsu, China), and visualized under a fluorescence microscope (Olympus, Tokyo, Japan) at an excitation wavelength of 350 nm and an emission wavelength of 460 nm.

Detection of intracellular ROS level. The production of peroxides was assessed using the ROS assay kit (Beyotime, Haimen, China). Briefly, SGC-7901 cancer cells were treated with 3-BrPA, SCT and 5-FU for 4 h, incubated with 10 μM DCFH-DA in serum-free medium at 37˚C for 20 min. Subsequently, the cells were imaged with a laser scanning confocal microscope (Nikon A1; Nikon Corporation, Tokyo, Japan) at excitation and emission wavelengths of 488 and 525 nm, respectively. The fluorescence intensity was regarded as the generation of ROS.

Establishment of a gastric carcinoma orthotopic xenograft model. Four-week-old female BALB/c athymic nude mice, weighing 20±2 g, were obtained from the Animal Experimental Center of Guangxi Medical University (Guangxi, China) and fed under specific pathogen-free conditions. All experimental procedures were conducted in accordance with the internationally recognized guidelines for conduct and animal welfare.

Mice were subcutaneously injected with 200 μl of suspension ($2x10^6$ cells/ml) of the SGC-7901 cell line in the back of axillary regions and sacrificed by cervical dislocation after 14 days when the palpable tumor diameter reached 1.0 cm. Tumor tissues were stripped and minced to 1-2 mm^3, and then transplanted into the next new group of mice for 6 sequential generations. The sixth subcutaneously transplanted tumor was used as the source of orthotopic transplantation.

Nude mice were anesthetized with sodium pentobarbital (45 mg/kg of body weight) by intraperitoneal injection, and an incision was made to carefully expose the stomach. The seromuscular layer of greater curvature was punctured with a needle to form a local concave niche where a tumor mass of ~1.0 mm^3 with good conditioning was imbedded and then the surface and greater omentum was covered with medical OB glue.

After transplantion for 2 weeks, 96 mice were randomly divided into the following 8 groups (n=12): control group (PBS, 10 ml/kg), 5-FU group (5-FU, 10 mg/kg), 3-BrPA low-dose group (3-BrPA-L, 1.85 mg/kg), 3-BrPA medium-dose group (3-BrPA-M, 2.23 mg/kg), 3-BrPA high-dose group (3-BrPA-H, 2.67 mg/kg), SCT low-dose group (SCT-L, 7.5 mg/kg), SCT medium-dose group (SCT-M, 15 mg/kg), and SCT high-dose group (SCT-H, 30 mg/kg). Nude mice were daily intraperitoneally injected with corresponding drugs or PBS (10 ml/kg), respectively. For 4 weeks the physical, stool and abdominal conditions of nude mice were observed throughout this experiment. After a 4-week treatment, half of the nude mice in each group were imaged with a micro-PET/CT scanner and then sacrificed by cervical dislocation. The tumor tissues and organs were stripped for subsequent studies. The remaining mice were continually treated until their death in order to evaluate the life prolonging rate.

Small-animal ^{18}F-FDG PET/CT scanning. A small-animal PET/CT scanner (Inveon; Siemens Medical Solutions,

Knoxville, TN, USA) was used for *in vivo* imaging. The SGC-7901 tumor-bearing mice were anesthetized with isoflurane (2% in 98% oxygen), kept at 38˚C and the caudal vein was injected with ^{18}F-FDG (5.55 MBp, 150 μCi) 40 min prior to imaging. A PET scan for 15 min was conducted on the mice followed by a 5 min CT scan. Three-dimensional regions of interest (ROI) were drawn around the gastric tumors and the standardized uptake value was measured as the percentage of injected radioactivity dose/gram (% ID/g).

Hematoxylin and eosin and immunohistochemistry (IHC) staining. The harvested tumor tissues, livers and kidneys were embedded in paraffin, sectioned at 5-μm thickness and stained with hematoxylin and eosin (H&E) for examination by light microscopy.

In addition, immunohistochemical (IHC) staining was performed using antibodies for cleaved caspase-9 (1:100 dilution) and cleaved caspase-3 (1:400 dilution) (both from Cell Signaling Technology, Danvers, MA, USA). The expression of cleaved caspase-9 and cleaved caspase-3 were determined based on the cytoplasmic and nuclear staining. The results were scored according to the mean density (MD) by Image-Pro Plus 6.0 and evaluated by 2 pathologists.

Lactate, ATP and glycolytic enzyme assay. To detect the inhibitory effect on glycolysis of 3-BrPA and SCT *in vivo*, the lactate production, ATP content and the glycolytic enzyme activity (HK, PFK-1 and PK) were assessed using assay kits (Jiancheng, Nanjing, China). According to the manufacturer's instructions, the absorbance at 340 nm was assessed spectrophotometrically (UV-2450; Shimadzu, Kyoto, Japan) and the results were calibrated with cellular protein concentration.

Western blot analysis. Total proteins were extracted from orthotopic tumors, electrophoresed in sodium dodecyl sulphate-polyacrylamide gel electrophoresis (SDS-PAGE), and then transferred onto a nitrocellulose filter membrane (Millipore, Billerica, MA, USA). Non-specific binding was blocked with 5% skimmed milk for 2 h at room temperature and incubation followed with specific primary antibodies at 4˚C overnight. The primary antibodies used were rabbit antibodies against Bax, Bcl-2, Cyt-C, survivin and GAPDH (1:1,000 dilution; Cell Signaling Technology). The anti-rabbit IgG DyLight 800-conjugated antibody was incubated at room temperature for 90 min (1:1,000 dilution; Cell Signaling Technology). The protein bands were visualized and quantified using the Odyssey system (LI-COR Biosciences, Lincoln, NE, USA).

Results

Drug sensitivity of cell lines. As shown in Table I, the IC_{50} values of 3-BrPA, SCT or 5-FU in the SGC-7901 GC cell line were 10.23±2.37 μg/ml and 7.19±1.05 mg/ml at 24 h, 6.15±1.24 μg/ml and 4.12±0.87 mg/ml at 48 h, 0.38±0.05 and 0.25±0.03 mmol/l at 48 h respectively.

Apoptosis is assessed by Hochest 33258 staining. The apoptotic cells, characterized by chromatin condensation and fragmentation, were observed after exposure to 3-BrPA and SCT for 24 h (Fig. 1A and C). The percentage of apoptotic cells increased along with the concentrations of 3-BrPA and SCT. The results strongly indicated that 3-BrPA and SCT induced SGC-7901 cell apoptosis *in vitro*.

Table I. IC_{50} values of 3-BrPA, SCT and 5-FU in the SGC-7901 cancer cell line *in vitro*.

Groups	3-BrPA (μg/ml)	SCT (mg/ml)	5-FU (mmol/l)
24 h	10.23±2.37	7.19±1.05	0.38±0.05
48 h	6.15±1.24	4.12±0.87	0.25±0.03

The results are expressed as the mean ± SD. 3-BrPA, 3-bromopyruvate; SCT, sodium citrate, 5-FU, 5-fluorouracil.

ROS is generated after 3-BrPA and SCT treatment. Intracellular ROS generation was evaluated using intracellular peroxide-dependent oxidation of DCFH-DA to form fluorescent DCF and detected with laser scanning confocal microscope after treatment with 3-BrPA and SCT for 4 h (Fig. 1B). ROS production was significantly increased upon treatment with 3-BrPA, SCT and 5-FU compared with the control (Fig. 1D; $p<0.05$). Furthermore, the fluorescence intensity increased along with the dose of 3-BrPA and SCT.

Effect of 3-BrPA and SCT on gastric orthotopic xenograft tumors. Gastric orthotopic xenograft models were successfully built (Fig. 2A and B), and the effect of 3-BrPA and SCT on tumor growth and survival time in mice were investigated. The orthotopic xenograft tumors were identified by touch through the abdominal wall 10 days after transplantation and the tumor formation rate was ~95% and the mortality rate was 4%. The mice administered by intraperitoneal injection with 3-BrPA and SCT exhibited tumor growth inhibition compared with the control group (Table II) ($p<0.05$). Moreover, as shown in Fig. 2D, the survival time of mice increased in the 3-BrPA and SCT groups ($p<0.05$). The results demonstrated that 3-BrPA and SCT suppressed tumor growth and prolonged tumor-bearing mice survival time.

Histology assessment. In order to determine whether 3-BrPA and SCT had a toxic effect on mice, the histopathological changes in the liver and kidneys were observed by H&E staining. As shown in Fig. 2C, histological examination did not reveal any apparent abnormalities, indicating the safety of the 3-BrPA and SCT doses used in the present study. However, slight vacuolar changes and spotty necrosis in hepatocytes, hydropic changes and leukocyte infiltration in kidney cells were observed in the 5-FU-treated mice.

3-BrPA and SCT suppresses glycolytic activity in tumors as determined by micro-PET/CT imaging. PET/CT with ^{18}F-FDG is a non-invasive approach to detect the glycolytic activity, and the radiotracer accumulation (% ID/g) in tumor areas, reflecting the intensity of tumor glucose metabolism. In the present study, we observed a significantly decreased radioactivity uptake in the mice treated with 3-BrPA and SCT (Fig. 3)

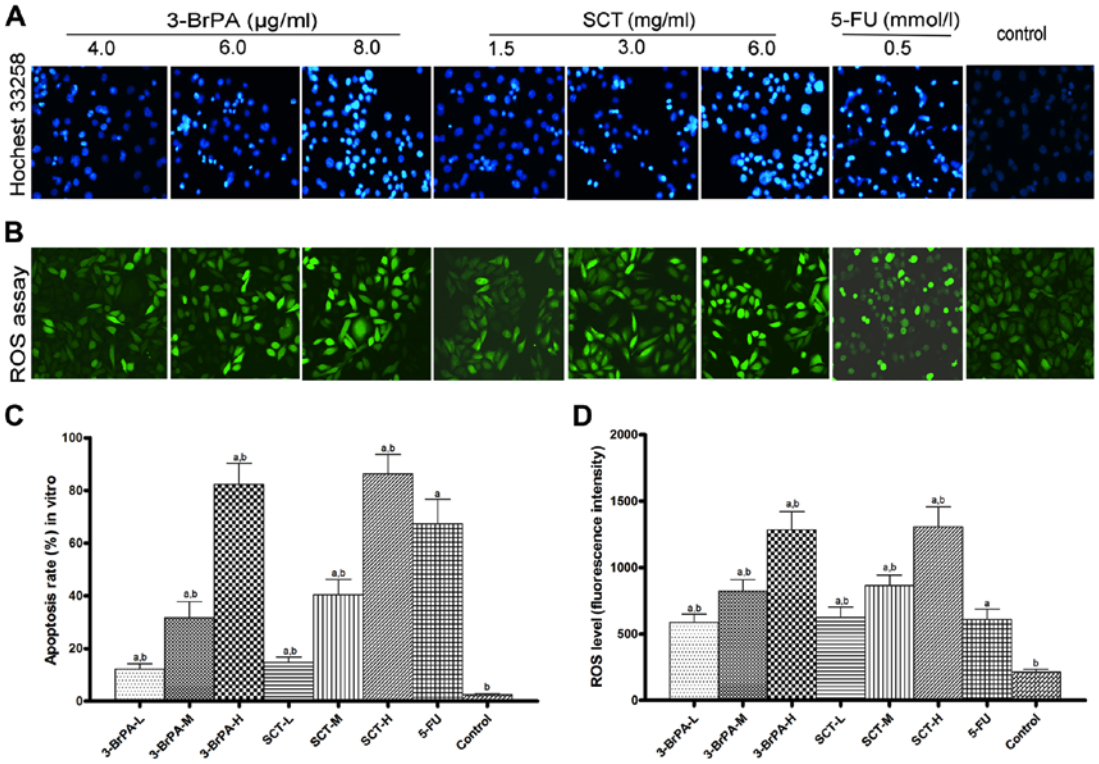

Figure 1. Effect of 3-BrPA and SCT on SGC-7901 cancer cells *in vitro*. (A and C) 3-BrPA and SCT induced SGC-7901 cell apoptosis *in vitro*. Under a fluorescence microscope, apoptotic cells stained with Hochest 33258 exhibited nucleic fragmentation and chromatin condensation. (B and D) 3-BrPA and SCT induced ROS generation in SGC-7901 cells. An increase in intracellular fluorescence intensity was detected in SGC-7901 cells by DCHF-DA assay using a laser scanning confocal microscope. The results are expressed as the mean ± standard deviation (n=3); ^{a}p<0.05 vs. the control; ^{b}p<0.05 vs. the 5-FU group. 3-BrPA, 3-bromopyruvate; SCT, sodium citrate; ROS, reactive oxygen species.

Table II. Results of nude mice weights, tumor volumes, tumor weights, and the inhibitory rate of tumors (%).

Group	Nude mice (n)	Tumor volume (mm^3)	Tumor weight (g)	Inhibitory rate of volume (%)	Inhibitory rate of weight (%)
3-BrPA-L	12	810.41±72.51	0.80±0.05	29.70±6.29^{a,b}	30.23±3.43^{a,b}
3-BrPA-M	12	730.08±60.10	0.70±0.04	36.67±5.21^{a,b}	39.43±5.09^{a,b}
3-BrPA-H	12	643.03±77.76	0.62±0.05	44.22±6.75^{a}	46.86±5.96^{a}
SCT-L	12	799.78±64.79	0.79±0.06	30.62±5.62^{a,b}	29.18±3.14^{a,b}
SCT-M	12	708.60±86.93	0.69±0.07	38.53±7.54^{a,b}	38.02±4.65^{a,b}
SCT-H	12	615.72±57.00	0.60±0.03	46.59±4.94^{a}	45.62±4.82^{a}
5-FU	12	605.48±61.53	0.60±0.05	47.48±5.34^{a}	47.04±5.07^{a}
Control	12	1152.77±88.99	1.13±0.08	0.00^{b}0.00^{b}	

The growth of orthotopic xenograft tumors in nude mice was markedly inhibited with 3-BrPA and SCT treatment (^{a}P<0.05). Results are presented as the mean ± standard deviation (n=12). ^{a}p<0.05 vs. control; ^{b}p<0.05 vs. 5-FU group. 3-BrPA, 3-bromopyruvate; SCT, sodium citrate, 5-FU, 5-fluorouracil.

(p<0.05), which may have resulted from the inhibition of PFK-1 and HK activities. Notably, a decrease of radiotracer accumulation was also observed in the 5-FU-treated group, which may be associated with the decrease of HK activity.

3-BrPA and SCT activate caspase cascades. Activation of caspase-3 and -9 is a key downstream event involved in the initiation and execution of apoptosis. From the IHC analysis (Fig. 4), the tumors from mice treated with 3-BrPA and SCT exhibited increased levels of cleaved caspase-3 and -9 in a dose-dependent manner, suggesting that the mechanism of apoptosis induced by 3-BrPA and SCT is related to caspase activation (p<0.05). Similarly, a significant increase in the expression of cleaved caspase-3 and -9 was also found in tumors with the 5-FU treatment.

Effects of 3-BrPA and SCT on Bcl-2, Cyt-C, Bax and survivin expression. To further investigate the possible underlying

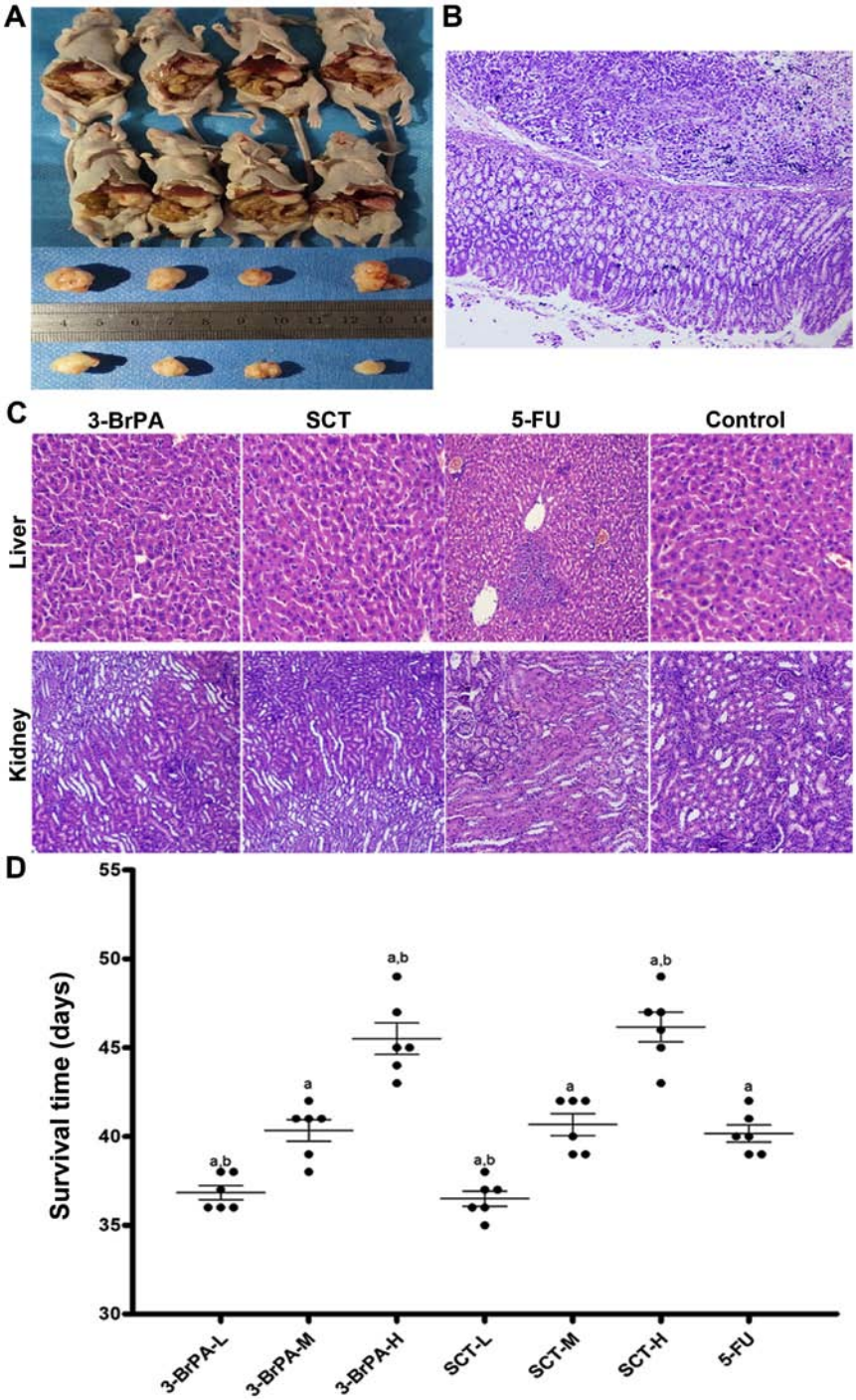

Figure 2. GC orthotopic xenograft tumors in nude mice are markedly inhibited by intraperitoneal injection of 3-BrPA and SCT. (A and B) We successfully built a GC orthotopic transplantation tumor model in nude mice. The weight and volume of the tumors in 3-BrPA, SCT and 5-FU-treated mice were significantly decreased ([a]p<0.05). (C) Microstructures of the liver and kidneys were observed by H&E staining. No significant pathological alterations were observed in the 3-BrPA and SCT-treated mice. (D) Intraperitoneal injection of 3-BrPA and SCT extended the survival time of tumor-bearing mice. Data are expressed as the mean ± SD (n=6); [a]p<0.05 vs. the control; [b]p<0.05 vs. the 5-FU group. GC, gastric cancer; 3-BrPA, 3-bromopyruvate; SCT, sodium citrate; 5-FU, 5-fluorouracil.

mechanism responsible for executing 3-BrPA and SCT induced apoptosis, we analyzed the expression of Bcl-2, Bax, Cyt-C and survivin using western blot analysis (Fig. 5A). The 3-BrPA and SCT-treated groups exhibited an increased expression of pro-apoptotic factors, Bax and Cyt-C, and a decreased expression of anti-apoptotic factors, Bcl-2 and survivin, in a concentration-dependent manner (p<0.05). However, with 5-FU treatment, Bax and Cyt-C were also upregulated while Bcl-2 and survivin were downregulated (p<0.05). These results from western blot and IHC analyses indicated that the mechanism of induced apoptosis by 3-BrPA and SCT may be mediated by suppressing survivin and activating the mitochondria-dependent pathway.

3-BrPA and SCT inhibit the activities of glycolytic enzymes to decrease lactate and ATP production. To further explore the potential mechanisms involved in the regulation of glucose metabolism of 3-BrPA and SCT *in vivo*, the activities of

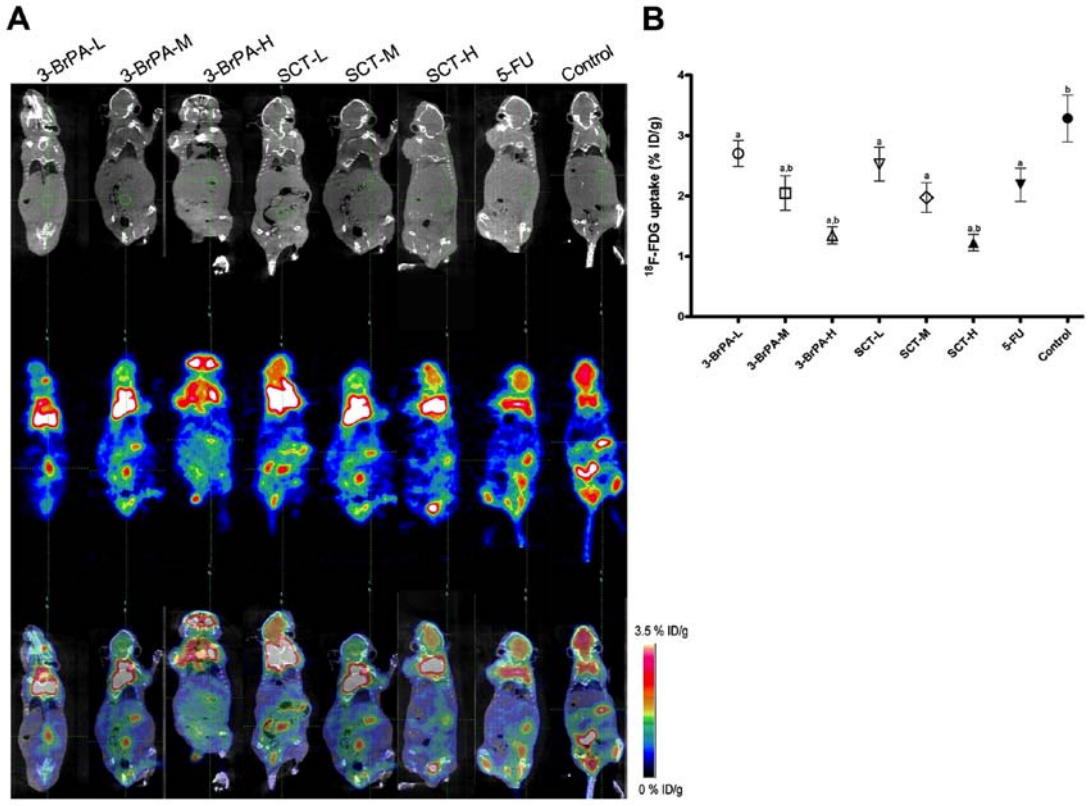

Figure 3. Micro-PET/CT scanning. (A) The coronal planes of nude mice with gastric orthotopic transplanted tumors were scanned by ^{18}F-FDG PET/CT (from top to bottom: CT, PET and PET/CT images). (B) Mice with a marked decrease in the uptake of ^{18}F-FDG were observed in the 3-BrPA and SCT-treated groups, which revealed the glycolytic activity and progression of tumors. The results are presented as the mean ± standard deviation from 5 independent mice; $^{a}p<0.05$ vs. the control; $^{b}p<0.05$ vs. the 5-FU group. 5-FU, 5-fluorouracil.

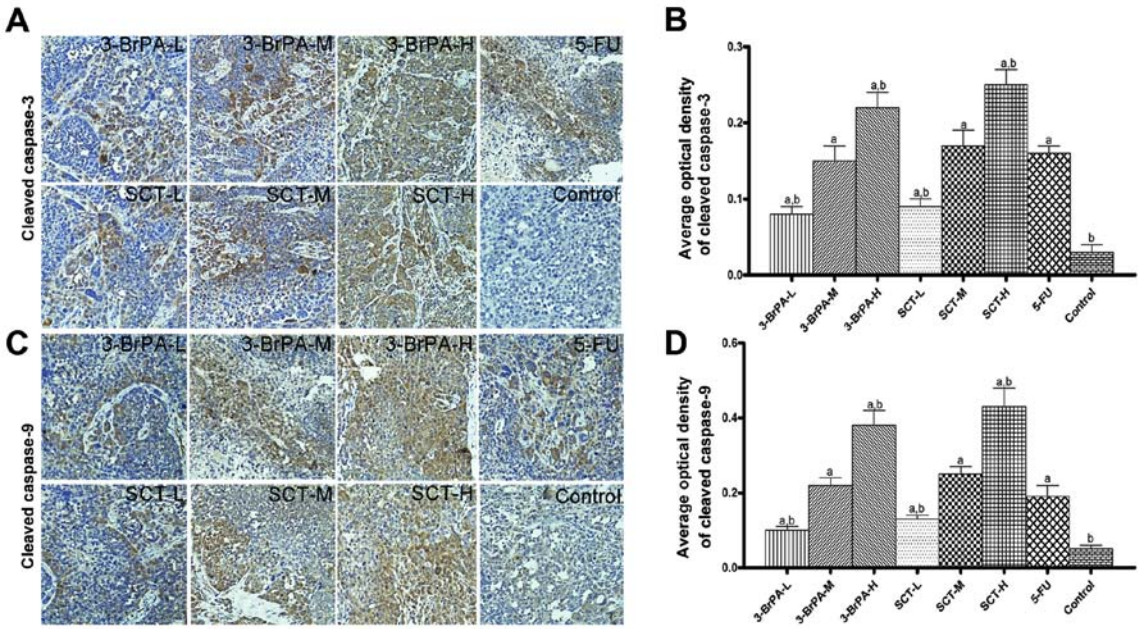

Figure 4. 3-BrPA and SCT significantly increase the protein expression of cleaved caspase-3 and -9 in tumor tissues. (A and B) IHC staining assay revealed that the expression of cleaved caspase-3 was increased in a dose-dependent manner after 3-BrPA and SCT treatment ($^{a}p<0.05$). (C and D) The expression of cleaved caspase-9 was also upregulated in the 3-BrPA, SCT and 5-FU groups ($^{a}p<0.05$). The results are presented as the mean ± standard deviation (n=6); $^{a}p<0.05$ vs. the control; $^{b}p<0.05$ vs. the 5-FU group. 3-BrPA, 3-bromopyruvate; SCT, sodium citrate; 5-FU, 5-fluorouracil.

glycolytic enzymes (PK, HK and PFK-1), lactate and ATP production in tumor tissues was assessed (Fig. 5B and C). The data revealed that lactate and ATP production was decreased in the 3-BrPA-treated group by suppression of HK activity, and it was also decreased in the SCT-treated group by inhibition of PFK-1 activity. Lactate and ATP production in the 5-FU-treated

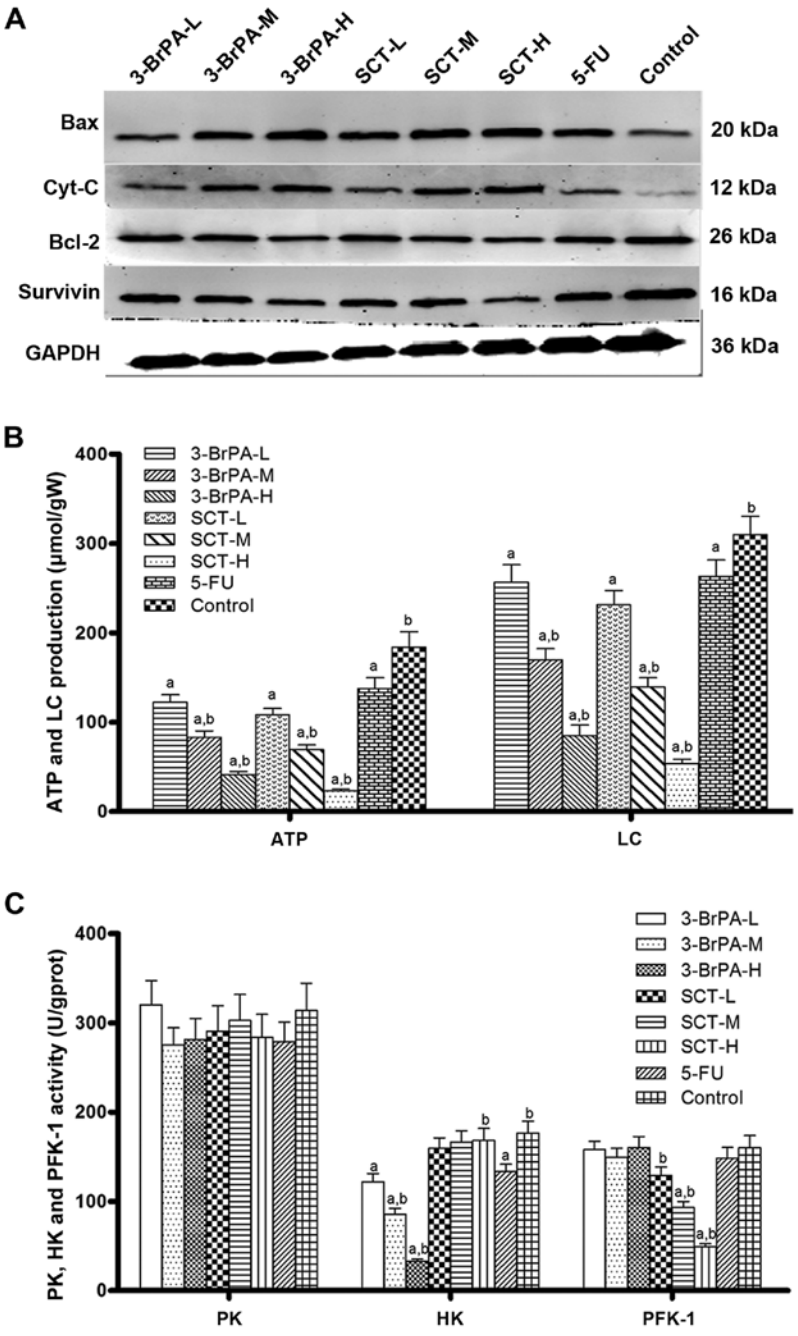

Figure 5. Analysis of the efficacy of 3-BrPA and SCT on apoptosis and glycolysis. (A) Results from western blot analysis revealed that the expression of Bax and Cyt-C were upregulated, and the expression of Bcl-2 and survivin were downregulated in the 3-BrPA and SCT-treated mice. (B) The production of lactate and ATP in the 3-BrPA and SCT-treated mice were significantly lower than in the PBS groups ($^{a}p<0.05$). (C) 3-BrPA and SCT can inhibit the activity of HK and PFK-1, respectively. However, the activity of PK exhibited no significant differences in all the groups ($p>0.05$). Data are expressed as the mean ± SD (n=6); $^{a}p<0.05$ vs. the control; $^{b}p<0.05$ vs. the 5-FU group. 3-BrPA, 3-bromopyruvate; SCT, sodium citrate; 5-FU, 5-fluorouracil, Cyt-C, cytochrome *c*.

group was significantly lower in contrast to the PBS group ($p<0.05$). Moreover, the activity of HK and PFK-1 was suppressed by 3-BrPA and SCT in a concentration-dependent manner, respectively.

Discussion

As discovered by Warburg 80 years ago, most malignant cells preferentially utilize glycolysis rather than oxidative phosphorylation for energy production even in the presence of oxygen (3) although the energy generation of glycolysis is far less efficient than oxidative phosphorylation (2 ATPs/glucose in glycolysis, but 36 ATPs from oxidative phosphorylation). However, increased glycolysis not only provides faster ATP production, but also greater lactic acid for tumor cell proliferation and invasion and may promote their resistance to chemoradiotherapy (3,7,26). Due to the altered metabolism in malignant cells, targeting glycolysis may provide a novel approach in the treatment of cancer.

A variety of agents have been explored to selectively suppress glycolysis. Some representative examples are DCA, 2-deoxyglucose, IAA and 3-BrPA. DCA activates the pyruvate

dehydrogenase complex by targeting pyruvate dehydrogenase kinase (27). 2-Deoxyglucose can non-competitively inhibit hexokinase II to block glycolysis (28). IAA is reported to inhibit glyceraldehyde-3-phosphate dehydrogenase and 6-phosphogluconate dehydrogenase (29). However, the exact underlying molecular mechanisms of these drugs are still under further investigation. Previous studies from Pedersen and our team had revealed that 3-BrPA decreased the glycolysis rate by suppressing mitochondrial hexokinase activity (9,10). Similarly, SCT has also been revealed to inhibit medullary thyroid cancer, leucocythemia, malignant pleural mesothelioma and ovarian carcinoma growth (10-13). On account of their potential ability in the treatment of malignant tumors, we employed 3-BrPA and SCT in the present study and attempted to reveal their underlying antitumor mechanisms. As shown in Fig. 5B and C, 3-BrPA and SCT decreased lactate and ATP production by targeting HK and PFK-1, respectively. The decrease of ATP and lactate may contribute to decrease the energy supply and disrupt the acidic microenvironment, resulting in tumor growth inhibition and apoptosis induction (Figs. 2 and 4).

In addition, based on the high glycolytic rates in malignant cancer, PET imaging with ^{18}F-FDG has been extensively used for clinical detection of tumors (30). Moreover, small animal PET/CT imaging has been frequently utilized to detect, monitor metastasis and evaluate therapeutic response in animal experiments (31,32). Due to the aforementioned rationale, in the present study, micro-PET/CT was employed to detect the accumulation of ^{18}F-FDG in gastric orthotopic xenografts to reflect their metabolic activity and viability. As shown in Fig. 3, the ^{18}F-FDG uptake decreased in the 3-BrPA, SCT and 5-FU-treated groups. The changes in radioactivity uptake were significantly correlated with the inhibition of HK and PFK-1 activities (Fig. 5C). In view of these results we suggest that a decrease in the uptake of ^{18}F-FDG reflects the glycolysis inhibition of tumors.

Apoptosis, known as a programmed cell death, is frequently utilized to evaluate the potential anticancer ability of a new therapeutic approach (33). To understand the effect on the apoptosis of 3-BrPA and SCT, we employed Hoechst 33258 staining. From the results of the Hoechst 33258 staining, we found that apoptosis was induced by 3-BrPA and SCT in a time- and concentration-dependent manner *in vitro* (Fig. 1A and C). In addition, the results of a TUNEL staining experiment in our previous study also indicated that 3-BrPA and SCT promote tumor cell apoptosis in a dose-dependent manner *in vivo* (9). Moreover, the typical morphological features of cell apoptosis were observed by TEM (9), and further demonstrated that 3-BrPA and SCT could induce apoptosis with intraperitoneal administration.

It is well known that there are 2 major signaling pathways that trigger apoptosis in mammalian cells: the extrinsic (death receptor) pathway and the intrinsic (mitochondrial) pathway. The extrinsic pathway can immediately activate caspase-8 by death receptors on the cell surface. However, in the intrinsic pathway, the Bcl-2 family modulates the mitochondrial membrane potential to regulate mitochondrial apoptotic signaling (18). Pro-apoptotic Bax promotes permeabilization of the outer mitochondrial membrane, induces the release of apoptogenic proteins such as cytochrome *c* (Cyt-C) into the cytoplasm and subsequent activation of caspase-9 (14-16). Conversely, anti-apoptotic Bcl-2 can negatively regulate the activity of Bax to inhibit apoptosis. Thus, the expression of Bax, Bcl-2 and Cyt-C proteins in tumors was assessed by western blot analyses. Our results indicated that when treated with increasing levels of 3-BrPA and SCT, the expression of the Bax and Cyt-C proteins gradually increased, while the expression of the Bcl-2 protein gradually decreased (Fig. 5A).

Moreover, the Cyt-C release from the mitochondria into the cytosol, forms apoptosomes with Apaf-1 and caspase-9, which ultimately activates caspase-3 (34). Activated caspase-9 could be regarded as an indicator of the mitochondrial-mediated apoptotic pathway and activated caspase-3 is the intersection of the extrinsic and intrinsic pathways. Both play critical roles in the execution of apoptosis (17). In the present study, the expression levels of cleaved caspase-9 and -3 were assessed by IHC staining. As shown in Fig. 4, 3-BrPA and SCT expedited the activation of caspase-9 and -3 in a concentration-dependent manner.

It is believed that the generation of ROS can cause uncontrolled oxidative stress, alter the mitochondrial membrane potential and activate caspase-9 to induce subsequent cell apoptosis (22,35,36). Increasing levels of ROS generated in the SGC-7901 cells were observed after a dose-increase of 3-BrPA and SCT treatment (Fig. 1B and D). Combined with the increased expression of Cyt-C, cleaved caspase-9 and -3 in tumor tissues, we speculated that ROS acted as upstream signaling molecules and played an important role in the induction of apoptosis.

In addition, as a member of the IAP family, survivin is abundantly expressed in the majority of human cancers, and numerous studies have revealed that it acts as a critical inhibitor of apoptosis to promote tumor proliferation and treatment resistance (19,37). Furthermore, survivin can inhibit the activation of caspases by directly binding to caspase-9 and -3 (20,21). As shown in Fig. 5A, a marked decrease of survivin in tumors was observed after treatment, which resulted in the upregulation of cleaved caspase-9 and -3. Thus, one of the antitumor mechanisms of 3-BrPA and SCT may rely on the inhibition of survivin to induce apoptosis.

To the best of our knowledge, this is the first demonstration that intraperitoneal injection of 3-BrPA and SCT leads to glycolysis restraint in gastric orthotopic xenografts and that this method is non-invasive and detectable by ^{18}F-FDG PET/CT. The results encourage the application of ^{18}F-FDG PET/CT to detect glycometabolism changes in tumors after treatment, as a considerable strategy to evaluate therapeutic response in pre-clinical research of malignant tumors. Furthermore, the present study revealed the underlying antitumor mechanisms of 3-BrPA and SCT, by suppressing the activities of glycolytic enzymes to decrease ATP and lactate production; increasing generation of ROS, downregulating the expression of survivin and inducing mitochondrial-mediated apoptosis. In addition, no significant pathological alterations in the liver and kidneys were observed after treatment, indicating the low toxicity of 3-BrPA and SCT. Collectively, our findings highlight the potential of intraperitoneal injection of 3-BrPA and SCT as a safe, novel and attractive strategy in gastric cancer treatment.

Acknowledgements

The present study was supported by the National Natural Science Foundation of China (grant no. 81260366), and The Guangxi Scientific Research and Technology Development Project.

References

1. Siegel RL, Miller KD and Jemal A: Cancer statistics, 2015. CA Cancer J Clin 65: 5-29, 2015.
2. Torre LA, Bray F, Siegel RL, Ferlay J, Lortet-Tieulent J and Jemal A: Global cancer statistics, 2012. CA Cancer J Clin 65: 87-108, 2015.
3. Vander Heiden MG, Cantley LC and Thompson CB: Understanding the Warburg effect: The metabolic requirements of cell proliferation. Science 324: 1029-1033, 2009.
4. Park MJ, Lee WJ, Lim HK, Park KW, Choi JY and Kim BT: Detecting recurrence of gastric cancer: The value of FDG PET/CT. Abdom Imaging 34: 441-447, 2009.
5. Weber WA and Wieder H: Monitoring chemotherapy and radiotherapy of solid tumors. Eur J Nucl Med Mol Imaging 33 (Suppl 1): S27-S37, 2006.
6. Najafov A and Alessi DR: Uncoupling the Warburg effect from cancer. Proc Natl Acad Sci USA 107: 19135-19136, 2010.
7. Zhao Y, Butler EB and Tan M: Targeting cellular metabolism to improve cancer therapeutics. Cell Death Dis 4: e532, 2013.
8. Pedersen PL: Warburg, me and Hexokinase 2: Multiple discoveries of key molecular events underlying one of cancers' most common phenotypes, the 'Warburg Effect', i.e., elevated glycolysis in the presence of oxygen. J Bioenerg Biomembr 39: 211-222, 2007.
9. Wang TA, Zhang XD, Guo XY, Xian SL and Lu YF: 3-Bromopyruvate and sodium citrate target glycolysis, suppress survivin, and induce mitochondrial-mediated apoptosis in gastric cancer cells and inhibit gastric orthotopic transplantation tumor growth. Oncol Rep 35: 1287-1296, 2016.
10. Kruspig B, Nilchian A, Orrenius S, Zhivotovsky B and Gogvadze V: Citrate kills tumor cells through activation of apical caspases. Cell Mol Life Sci 69: 4229-4237, 2012.
11. Lincet H, Kafara P, Giffard F, Abeilard-Lemoisson E, Duval M, Louis MH, Poulain L and Icard P: Inhibition of Mcl-1 expression by citrate enhances the effect of Bcl-x_L inhibitors on human ovarian carcinoma cells. J Ovarian Res 6: 72, 2013.
12. Halabe Bucay A: Hypothesis proved...citric acid (citrate) does improve cancer: A case of a patient suffering from medullary thyroid cancer. Med Hypotheses 73: 271, 2009.
13. Lu Y, Zhang X, Zhang H, Lan J, Huang G, Varin E, Lincet H, Poulain L and Icard P: Citrate induces apoptotic cell death: A promising way to treat gastric carcinoma? Anticancer Res 31: 797-805, 2011.
14. Jin Z and El-Deiry WS: Overview of cell death signaling pathways. Cancer Biol Ther 4: 139-163, 2005.
15. Ghobrial IM, Witzig TE and Adjei AA: Targeting apoptosis pathways in cancer therapy. CA Cancer J Clin 55: 178-194, 2005.
16. Fulda S and Debatin KM: Extrinsic versus intrinsic apoptosis pathways in anticancer chemotherapy. Oncogene 25: 4798-4811, 2006.
17. Slee EA, Adrain C and Martin SJ: Executioner caspase-3, -6, and -7 perform distinct, non-redundant roles during the demolition phase of apoptosis. J Biol Chem 276: 7320-7326, 2001.
18. Taylor RC, Cullen SP and Martin SJ: Apoptosis: Controlled demolition at the cellular level. Nat Rev Mol Cell Biol 9: 231-241, 2008.
19. Mita AC, Mita MM, Nawrocki ST and Giles FJ: Survivin: Key regulator of mitosis and apoptosis and novel target for cancer therapeutics. Clin Cancer Res 14: 5000-5005, 2008.
20. Shin S, Sung BJ, Cho YS, Kim HJ, Ha NC, Hwang JI, Chung CW, Jung YK and Oh BH: An anti-apoptotic protein human survivin is a direct inhibitor of caspase-3 and -7. Biochemistry 40: 1117-1123, 2001.
21. Tamm I, Wang Y, Sausville E, Scudiero DA, Vigna N, Oltersdorf T and Reed JC: IAP-family protein survivin inhibits caspase activity and apoptosis induced by Fas (CD95), Bax, caspases, and anticancer drugs. Cancer Res 58: 5315-5320, 1998.
22. Orrenius S, Gogvadze V and Zhivotovsky B: Mitochondrial oxidative stress: Implications for cell death. Annu Rev Pharmacol Toxicol 47: 143-183, 2007.
23. Sausv ille EA, Burg er AM: Contributions of human tumor xenografts to anti cancer drug development. Cancer Res 66: 3351-3354, 2006.
24. Johnson JI, Decker S, Zaharevitz D, Rubinstein LV, Venditti JM, Schepartz S, Kalyandrug S, Christian M, Arbuck S, Hollingshead M, *et al*: Relationships between drug activity in NCI preclinical in vitro and in vivo models and early clinical trials. Br J Cancer 84: 1424-1431, 2001.
25. Bibby MC: Orthotopic models of cancer for preclinical drug evaluation: Advantages and disadvantages. Eur J Cancer 40: 852-857, 2004.
26. Solaini G, Sgarbi G and Baracca A: Oxidative phosphorylation in cancer cells. Biochim Biophys Acta 1807: 534-542, 2011.
27. Bonnet S, Archer SL, Allalunis-Turner J, Haromy A, Beaulieu C, Thompson R, Lee CT, Lopaschuk GD, Puttagunta L, Bonnet S, *et al*: A mitochondria-K^+ channel axis is suppressed in cancer and its normalization promotes apoptosis and inhibits cancer growth. Cancer Cell 11: 37-51, 2007.
28. Singh D, Banerji AK, Dwarakanath BS, Tripathi RP, Gupta JP, Mathew TL, Ravindranath T and Jain V: Optimizing cancer radiotherapy with 2-deoxy-d-glucose dose escalation studies in patients with glioblastoma multiforme. Strahlenther Onkol 181: 507-514, 2005.
29. Fahim FA, Esmat AY, Mady EA and Ibrahim EK: Antitumor activities of iodoacetate and dimethylsulphoxide against solid Ehrlich carcinoma growth in mice. Biol Res 36: 253-262, 2003.
30. Buerkle A and Weber WA: Imaging of tumor glucose utilization with positron emission tomography. Cancer Metastasis Rev 27: 545-554, 2008.
31. Bradbury MS, Hambardzumyan D, Zanzonico PB, Schwartz J, Cai S, Burnazi EM, Longo V, Larson SM and Holland EC: Dynamic small-animal PET imaging of tumor proliferation with 3'-deoxy-3'-^{18}F-fluorothymidine in a genetically engineered mouse model of high-grade gliomas. J Nucl Med 49: 422-429, 2008.
32. Walter MA, Hildebrandt IJ, Hacke K, Kesner AL, Kelly O, Lawson GW, Phelps ME, Czernin J, Weber WA and Schiestl RH: Small-animal PET/CT for monitoring the development and response to chemotherapy of thymic lymphoma in *Trp53*$^{-/-}$ mice. J Nucl Med 51: 1285-1292, 2010.
33. Talib WH and Mahasneh AM: Antiproliferative activity of plant extracts used against cancer in traditional medicine. Sci Pharm 78: 33-45, 2010.
34. Launay S, Hermine O, Fontenay M, Kroemer G, Solary E and Garrido C: Vital functions for lethal caspases. Oncogene 24: 5137-5148, 2005.
35. Gupta S, Yel L, Kim D, Kim C, Chiplunkar S and Gollapudi S: Arsenic trioxide induces apoptosis in peripheral blood T lymphocyte subsets by inducing oxidative stress: A role of Bcl-2. Mol Cancer Ther 2: 711-719, 2003.
36. Fan TJ, Han LH, Cong RS and Liang J: Caspase family proteases and apoptosis. Acta Biochim Biophys Sin 37: 719-727, 2005.
37. Church DN and Talbot DC: Survivin in solid tumors: Rationale for development of inhibitors. Curr Oncol Rep 14: 120-128, 2012.